https://doi.org/10.5194/egusphere-2024-1776
Preprint. Discussion started: 20 June 2024

Responses of microbial metabolic rates to non-equilibrated silicate vs calcium-based ocean alkalinity enhancement

Laura Marín-Samper[1], Javier Arístegui[1], Nauzet Hernández-Hernández[1], Ulf Riebesell[2]

[1] Instituto de Oceanografía y Cambio Global, Universidad de Las Palmas de Gran Canaria, 35017 Telde, Spain
[2] GEOMAR Helmholtz Centre for Ocean Research Kiel, 24148 Kiel, Germany

Correspondence to: Laura Marín-Samper (laura.marin@ulpgc.es), Javier Arístegui (javier.aristegui@ulpgc.es)

Abstract. This study contributes to the inaugural exploration of non-equilibrated Ocean Alkalinity Enhancement (OAE). The manipulation of Total Alkalinity (TA), involving silicate and calcium-based ΔTA gradients ranging from 0 to 600 µmol · L^{-1}, was conducted without prior CO_2 sequestration, under natural conditions and at a mesocosm scale (~60 m^3). The resulting impact included an increase in pH and a decrease in pCO_2, sustained across the experiment, as full natural equilibration via sea-gas exchange did not occur. Implemented in a neritic system under post-bloom conditions, a midway mixing event was simulated. Following an inorganic nutrient addition, discernible delays in bloom formation, as indicated by the Gross Production (GP) and Net Community Production (NCP) rates, as well as by the chlorophyll-a (Chla) concentrations, in relation to the ΔTA gradient, were observed. Notably, the delay was more pronounced for the calcium treatment set compared to the silicate one, where low TA treatments exhibited earlier responses than high TA ones. This delay is likely attributed to the previously documented, species-specific negative relationships between high pH/lowCO_2 levels and phytoplankton growth rates. This study underscores the need for further investigation into the implications of this response pattern in terms of trophic transfer and seasonal suitability. Further, it is anticipated that a wider delay in bloom formation would be evident with a larger non equilibrated TA gradient. Thus, highlighting the importance of exploring variations in TA limits for a comprehensive understanding of the OAE's impacts.

Keywords. OAE, alkalinization, silicate-based, calcium-based, community production, metabolic rates

1. Introduction

To reduce the concentration of atmospheric carbon dioxide (CO_2), and to be able to stay below the 1.5 to 2 ºC global mean temperature increase relative to preindustrial times, the realistic emissions cut alone is projected not to be sufficient (Friedlingstein et al., 2022, 2019; Fuss et al., 2020; IPCC, 2018, 2023; Lee et al., 2021). The changes to our technological and socio-economic systems that would be necessary to attain the required emissions reductions can take decades, or longer, to be implemented (Renforth and Henderson, 2017). In fact, all the projections that simulate the agreed upon conditional and unconditional Nationally Determined Contributions (NDCs) in terms of emissions cuts, and that also assume gross negative emissions, still fall well above those in which the temperature is restricted to the targeted maximum increase (IPCC, 2023). The latter require more extensive emissions reductions, alongside reaching net-zero emissions by 2050, and net negative emissions for the rest of the century (IPCC, 2018, 2023). Therefore, the need for atmospheric carbon removal and sequestration is imperative to avoid the serious, long-term

https://doi.org/10.5194/egusphere-2024-1776
Preprint. Discussion started: 20 June 2024

climatic consequences associated with surpassing the aforementioned temperature limit, which is considered a tipping point.

Ocean alkalinity enhancement (OAE) is a marine carbon dioxide removal (mCDR) approach that shows great promise. Model studies indicate that OAE shows the potential to remove atmospheric carbon at a gigaton (Gt) scale annually (Feng et al., 2017; Harvey, 2008). Although it not only shows potential for carbon capture and long-term sequestration. It is also known to possibly aid in the allayment of ocean acidification (OA; Albright et al., 2016; Gattuso et al., 2018; Feng et al., 2017; Harvey, 2008). OAE is attained through the addition, in various ways, of alkali or alkaline compounds to seawater increasing total alkalinity (TA), pushing the carbonate equilibrium system from CO_2 to the bicarbonate (HCO_3^-) and carbonate (CO_3^{-2}) species (Kheshgi, 1995). This process allows for additional CO_2 diffusion in the course of regaining balance with the atmosphere and alleviates the effects of OA by increasing the ocean's buffering capacity.

CO_2 equilibration can be induced prior to the alkalinity addition, or the alkalinity plume can be left to equilibrate naturally through sea-gas exchange, which is more feasible. Indeed, large scale equilibrated OAE application would require the use of reactors to CO_2 equilibrate the alkaline solutions before deployment (Hartmann et al., 2023). If left to natural sea-gas exchange however, this process can take several months to years (Jones et al., 2014). Notably, when carbon dioxide is not chemically pre-sequestered, the alterations to the carbonate system become more prominent. These consist of a substantial decrease in CO_2 partial pressure (pCO_2) and a subsequent significant increase in pH, particularly when compared to methods involving pre-equilibration. Such reduced pCO_2 resulting from the alkalinity manipulation without prior equilibration could potentially lead to CO_2 limitation among phytoplankton (Riebesell et al., 1993).

Past studies have in fact reported taxon-specific responses in phytoplankton growth based on the combined effects of pCO_2 and H^+ concentration in the context of OA (e.g., Paul & Bach, 2020). Before OA became a central focus of scientific research, high pH/low CO_2 conditions were observed to cause declines in marine phytoplankton growth rates (Goldman, 1999; Hansen, 2002). Notably, under air equilibrated conditions, species-specific half saturation values ($k_{½}$) for HCO_3^- and CO_2 acquisition in photosynthesis have also been reported (Raven and Johnston, 1991). Hence, given that the utilization of non-equilibrated OAE will entail significant changes to said carbonate system parameters, a response in terms of microbial production rates in relation to the deployed non-equilibrated alkalinity gradient was expected.

Another factor of uncertainty when considering OAE implementation is the source mineral type, whether it is calcium or silicate based. For silicate based OAE deployment, olivine-rich minerals, such as dunite, which contain forsterite (Mg_2SiO_4), are being considered (Montserrat et al., 2017; Renforth and Henderson, 2017). This is because olivine occurs commonly in nature and weathers relatively quickly, eliminating the need for energy-intensive chemical processing prior to dissolution (Schuiling and Krijgsman, 2006; Renforth and Henderson, 2017). However, its dissolution releases silicon, which may benefit silicifiers (such as diatoms), and iron, which is a co-limiting micronutrient, but also other potentially harmful by-products such as nickel (Xin et al., 2023), and other trace metals (Bach et al., 2019).

https://doi.org/10.5194/egusphere-2024-1776
Preprint. Discussion started: 20 June 2024

A calcium-based mineral is being considered for OAE deployment is hydrated lime (Kheshgi, 1995). It is produced through the calcination of limestone and would dissolve much faster than any natural mineral (Renforth and Henderson, 2017). Besides, the latter does not contain any dissolution by-products that could in theory negatively impact biota. However, the introduction of calcium to the system may promote calcification (Albright et al., 2016; Bach et al., 2019), a process through which CO_2 is emitted (Zeebe and Wolf-Gladrow, 2001). Thus, that would entail a reduction in the OAE's carbon capture efficiency, alongside benefiting benthic (Albright et al., 2016) and potentially pelagic calcifiers, so possibly also inducing a plankton community composition shift away from silicifiers (Bach et al., 2019).

Considering all the aforementioned unknowns, the current study aimed at monitoring the response of the microbial community to a silicate versus a calcium-based, non-CO_2 equilibrated OAE implementation. To isolate the effects of the carbonate chemistry alterations in both case scenarios and to avoid confounding variables due to impurities in the raw minerals, simulations were employed. Compounds that separately contain the mentioned key elements present in hydrated lime and forsterite, already in solution, were used. Gross and net oxygen production rates, community respiration rates, metabolic balance, and chlorophyll *a* (Chl*a*) concentration were monitored over a ~10-week period. Alterations driven by the mineral type, and the carbonate chemistry changes to the mentioned rates were expected (Riebesell et al., 1993; Bach et al., 2019; Paul and Bach, 2020). Addressing the aforementioned knowledge gaps is key in understanding the non-equilibrated OAE's environmental impacts, its potential for CO_2 removal in terms of efficiency and long-term sequestration, and thus in choosing a suitable approach for its safe deployment.

2. MATERIALS AND METHODS

2.1 Experimental setup and sampling

The experiment (KOSMOS Bergen 2022) was carried out in Raunefjorden, 1.5 km offshore from the Espegrend Marine Research Field Station, of the University of Bergen, Norway, starting on the 7th of May 2022. This location provided protection from swells and access to all the necessary facilities to conduct the experiment right onshore (Ferderer et al., 2023). Ten KOSMOS (Kiel Offshore Mesocosms for Ocean Simulations; Riebesell et al., 2013) units, or mesocosms, of an approximately 60 m^3 capacity were deployed. The mesocosm cylindrical bags (20 m long and 2.5 m in diameter) were left submerged and opened at the bottom for approximately a week prior to the start of the experiment on the 13th of May. Therefore, allowing for enough open water exchange to enclose a natural planktonic community as homogeneously as possible amongst all mesocosms. To close them, the sediment traps (2 m long, funnel shaped) were placed on the bottom ends, the tops of the bags were drawn out 1m off the water's surface, and the mesocosm roofs were put in place. In order to exclude all unevenly allocated large organisms, a ring with the same diameter as the mesocosms (Riebesell et al., 2013), and with a 1 mm net attached to it, was pulled from bottom to top, just after mesocosm closure (Day 0). Two days after closure, the volume contained in the mesocosms was determined. To do that, the water inside the mesocosms was first homogenized using a spider-like dispensing device (named henceforth "spider", see Riebesell et al., 2013) to bubble compressed air up and down the water column. Later, by adding 50 L of brine solution, also using the spider, with a known concentration, and measuring salinity before and after said addition, the volume

https://doi.org/10.5194/egusphere-2024-1776
Preprint. Discussion started: 20 June 2024

contained in each mesocosm could be calculated, as in Czerny et al. (2013). Mesocosm inside and outside cleaning was carried out once a week. Outside cleaning was done by divers and people assisting from boats, using brushes. The inside cleaning was realized sinking a ring with the same diameter as the mesocosms, with rubber blades around its circumference, and pulling it up. This way removing any growth found in the mesocosm walls that could interfere with the results of the experiment.

Samples from the entire 20 m water column inside the mesocosms, and from the fjord, were collected every two days using Integrated Water Samplers (IWS III, HYDRO-BIOS Apparatebau GmbH, Altenholz, Germany) with a 5 L internal volume capacity. Mesocosms were sampled in a random order and an extra sample from the fjord was always taken from the same location right next to mesocosms 5. After three sampling days (day 6), to properly monitor the starting conditions, the TA manipulation was applied. The experiment ended on the 6th of July, lasting 53 days. For further information on all the research and maintenance activities carried out throughout the experimental period, please refer to Supp. Fig. S1.

2.2 Carbonate chemistry manipulation and nutrient fertilization

The mesocosms were divided into two sets of five (see Table 1). Out of one of these sets, four mesocosms were treated with $CaCl_2$, and with NaOH setting a Total Alkalinity (TA) gradient from ΔTA 0, in increments of 150 µmol · L^{-1}, up to a ΔTA of 600 µmol · L^{-1}. The other set of five were treated with $MgCl_2$, Na_2SiO_3, and with NaOH following the said TA gradient. The amount of Mg^{2+} and Ca^{2+} were increased in proportion to the NaOH addition, whereas the amount of Na_2SiO_3 added was the same (75 µmol·L^{-1} target concentration) in all the silicate based OAE treatments, including the control. The TA increase of 2:1 with respect to the amount of Na_2SiO_3 added was taken into consideration by reducing the amount of NaOH accordingly, and by adding diluted HCl in the silicate-based control (Ferderer, et al., 2023). The target amounts of NaOH, Na_2SiO_3 and $MgCl_2$, and $CaCl_2$ for each treatment were dissolved in 20 L of MiliQ water. These were later added to the mesocosms, evenly up and down the water column, using the spider.

An inorganic nutrient addition was carried out on day 26 due to the oligotrophic conditions found inside the mesocosms compared to those observed in the fjord. But also, because the community inside was close to reaching heterotrophic balance even though the light conditions were reasonably optimal. The nitrate (NO_3^-) target concentration was 4 µmol L^{-1}, phosphate (PO_4^{3-}) was added following the N:P Redfield ratio of 16:1 across all mesocosms, and silicate was added in an N: Si ratio of 4:1 only in the calcium treatments. A second addition on day 28 was undertaken to correct for stoichiometric differences between mesocosms (see Ferderer, et al., 2023).

2.2 Carbonate chemistry

Samples for TA, Dissolved Inorganic Carbon (DIC), and total seawater pH were collected into 250 mL glass flasks, allowing for plenty overflow, directly from the IWSs. TA and pH samples were collected every two days, whereas DIC was only measured on day 9. Samples were later sterile filtered (0.2 µm, SARSTEDT, Nümbrecht, Germany) with a peristaltic pump and with special care to avoid sea-gas exchange. TA concentrations were determined by a potentiometric two step titration using a Metrohm 862 Compact Titrosampler with HCl 0.05 M as the titrant, an Aquatrode Plus (Pt1000), and a 907 Titrando unit, as in Chen et al., 2022. DIC concentrations were measured with an AIRICA system (Marianda, Kiel,

https://doi.org/10.5194/egusphere-2024-1776
Preprint. Discussion started: 20 June 2024

Germany; see Gafar & Schulz, 2018, and Taucher et al., 2017) with a differential gas analyzer (LI-7000, LI-COR Biosciences GmbH, Bad Homburg, Germany) at room temperature and within 12 h. Also, total seawater pH samples were acclimated to 25ºC in a thermostatic bath and later measured spectrophotometrically, at the same temperature, with a VARIAN Cary 100 in a 10 cm cuvette (Dickson et al., 2007). The rest of the carbonate system parameters were calculated with CO2Sys v2.5 (Lewis and Wallace, 1998) using the measured TA, total seawater pH, and nutrient concentrations, as well as the in-situ temperature and salinity daily means obtained from the CTD casts (see Sup. Fig. S1). pH was corrected against the measured DIC on day 9.

2.3 Dissolved inorganic nutrient concentrations

Triplicate samples to account for technical variability were collected every two days. These were sterile filtered using 0.45 µm PES fiber syringe filters (Filtropur S, SARSTEDT, Nümbrecht, Germany) and kept in the dark and at ambient temperature until further processing. Nitrate (NO_3^-), nitrite (NO_2^-), phosphate (PO_4^{3-}), and silicate ($Si(OH)_4$) concentrations were determined spectrophotometrically as in Hansen & Koroleff (1999). Ammonia (NH_4^+) was measured using a 10-AU Fluorometer (TURNER designs, San Jose, CA, USA) following Holmes et al. (1999).

2.4 Metabolic rates through oxygen production and consumption

Gross Production (GP), Net Community Production (NCP), and Community Respiration (CR) rates were determined by oxygen production and consumption in calibrated 125 mL nominal volume soda lime glass bottles following the Winkler method and the recommendations from Carpenter (1966), Bryan et al. (1976), and Grasshof et al. (1999), also described by Marín-Samper et al. (2024). Polycarbonate bottles were filled with 4.5 L of seawater per mesocosm, and from the fjord on each sampling day directly from the IWSs and brought to the lab. Out of each 4.5 L sample, ten soda lime bottles were first rinsed with sample water and then randomly filled, allowing ample overflow, using a silicone tube with an attached 280 µm mesh on one end. Four out of the ten subsamples per mesocosm were fixed at the moment of collection, "initials", through the addition of 1 mL of a manganese chloride ($MnCl_2$) solution, and 1 mL of a sodium iodide (NaI) based alkaline solution, in this order. They were later covered with a blackout piece of fabric and stored upright in a rack underwater. Another three bottles were incubated inside opaque bags, namely "dark" ones, and the remaining three were incubated under "light" conditions. The latter were randomly distributed inside clear methacrylate incubators set outside, which were covered with a blue foil (172 Lagoon Blue foil, Lee filters, Burbank, USA) to better simulate the light spectrum of the water column, along with the "initials", and the bags containing the "dark" ones. The incubators were hooked to a constant water flow system that siphoned water directly out of the fjord (from 14 m depth), into the incubator, and out into the fjord again. Data loggers (HOBO UA-002-64, Australia/New Zealand) were placed inside the incubators to monitor the temperature (roughly 11.11 and 10.34 °C during the day and night, respectively) and light (ranging from 0.20 to 688.89 µmol photons m^{-2} s^{-1}) conditions throughout the experiment. After an incubation period of 24 hours, all samples were fixed and left to sediment for at least 2 hours. Finally, samples were acidified with 1 mL of 5 M sulphuric acid (H_2SO_4) and analysed with an automated titration system, with colorimetric end-point detection (Dissolved Oxygen Analyzer, SIS Schwentinental, Germany), using a 0.25 M sodium thiosulphate solution ($Na_2S_2O_3 * 5H_2O$) as the titrant. The mean of each

https://doi.org/10.5194/egusphere-2024-1776
Preprint. Discussion started: 20 June 2024

set of replicates was used to calculate CR, NCP, and GP rates, using the following Eq. (1), Eq. (2) and Eq. (3) respectively:

$$\mathrm{CR}\ [\mu\mathrm{mol\ L^{-1}h^{-1}}] = \frac{\mathrm{Conc_I - Conc_D}}{\mathrm{h_D}} \quad (1)$$

$$\mathrm{NCP}\ [\mu\mathrm{mol\ L^{-1}h^{-1}}] = \frac{\mathrm{Conc_L - Conc_I}}{\mathrm{h_L}} \quad (2)$$

$$\mathrm{GP}\ [\mu\mathrm{mol\ L^{-1}h^{-1}}] = \mathrm{CR} + \mathrm{NCP} \quad (3)$$

where $\mathrm{Conc_I}$, $\mathrm{Conc_D}$ and $\mathrm{Conc_L}$ correspond to the mean oxygen concentration of the initial, dark, and light samples, respectively. T stands for incubation time in hours. The metabolic balance was later calculated by dividing the obtained GP rates by the CR rates.

Due to a COVID outbreak in the base, the two scientists in charge of measuring this parameter had to be confined. Therefore, data were not collected on days 47 and 49.

2.5 Chlorophyll *a* concentration

Chlorophyll *a* (Chla) samples for each mesocosm were collected into 1000 mL dark bottles from 10L canisters that were filled directly from the IWSs. Samples were filtered through a 200 µm mesh. Chla concentration was determined fluorometrically after Welschmeyer (1994).

2.7 Data analysis

Data for days 47 and 49 for GP were calculated using the equation from a Spearman correlation model with Chla, with both variables transformed to base-10 logarithm. NCP rates for those two days were calculated using the equation obtained through also a Spearman correlation model of NCP with GP. The calculated NCP was then subtracted to the estimated GP to obtain CR for those two days. Daily linear regressions in relation to the target ΔTA were carried out to determine the evolution of the TA effect on production and respiration rates, and on the Chla concentration observed. To aid in the system's response interpretation, the experiment was divided into two phases: pre-nutrient addition phase (phase I: from day 7 to day 25), and a post-nutrient addition phase (phase II: from day 27 to day 53).

3. RESULTS

3.1 Carbonate chemistry and inorganic nutrient concentrations

The target TA gradient was achieved, albeit with small differences between the silicate and calcium based OAE treatments. The attained TA gradient was lower than the targeted levels, and, moving up said gradient, the mentioned differences slightly widened (Table 1). Additionally, TA, and thus also pCO_2 and pH, were marginally distinct between the meant to be equivalent, calcium and silicate-based treatments, particularly in the three highest ones (Figure 1).

https://doi.org/10.5194/egusphere-2024-1776
Preprint. Discussion started: 20 June 2024

Table 1. The first column corresponds to the mesocosms (MK), and next to it the source mineral type. The target ΔTotal Alkalinity (TA) gradient, in µEq · L^{-1}, is listed for each MK, with the measured or "attained" mean ΔTA, and finally the difference between the theoretical/target gradient and the actual mean ΔTA obtained.

MK	Mineral	Target ΔTA	Attained ΔTA	Target-Attained
M5	Ca	0	0	0
M1	Ca	150	138.4	11.6
M9	Ca	300	287.5	12.5
M7	Ca	450	404.0	46.0
M3	Ca	600	530.0	70.0
M6	Si	0	0	0
M10	Si	150	140.3	9.7
M2	Si	300	278.9	21.1
M4	Si	450	422.4	27.6
M8	Si	600	550.4	49.6

The mean pH levels obtained ranged from 8.06 ± 0.02 to 8.71 ± 0.03, and from 8.03 ± 0.02 to 8.72 ± 0.02, in the calcium and silicate treatments respectively (Figure 1 B). In terms of mean pCO_2, the difference between the controls and the highest treatments was quite steep, going from 372.3 ± 19.7 and 397.05 ± 20.4 µatm, in the calcium and silicate controls, down to 76.08 ± 7.4 and 72.6 ± 5.07 µatm in the highest treatments, correspondingly (Figure 1 C).

A noteworthy result is that full natural equilibration did not occur after a 53-day long experiment. CO_2 incursion was minor, as it is clear from the pH and pCO_2 levels included in Figure 1 B and C. In fact, when deducting the calculated pCO_2 levels obtained on day 53, to those right after the TA manipulation on day 7, differences fall between 75.98 and 12.75 µatm, and follow a declining gradient going from the ΔTA 0 treatments, to the highest ones (Supp. Table S1). Therefore, the pH and pCO_2 levels in the mesocosms where TA was manipulated never reached, nor got closer to, the levels observed in the "controls".

https://doi.org/10.5194/egusphere-2024-1776
Preprint. Discussion started: 20 June 2024

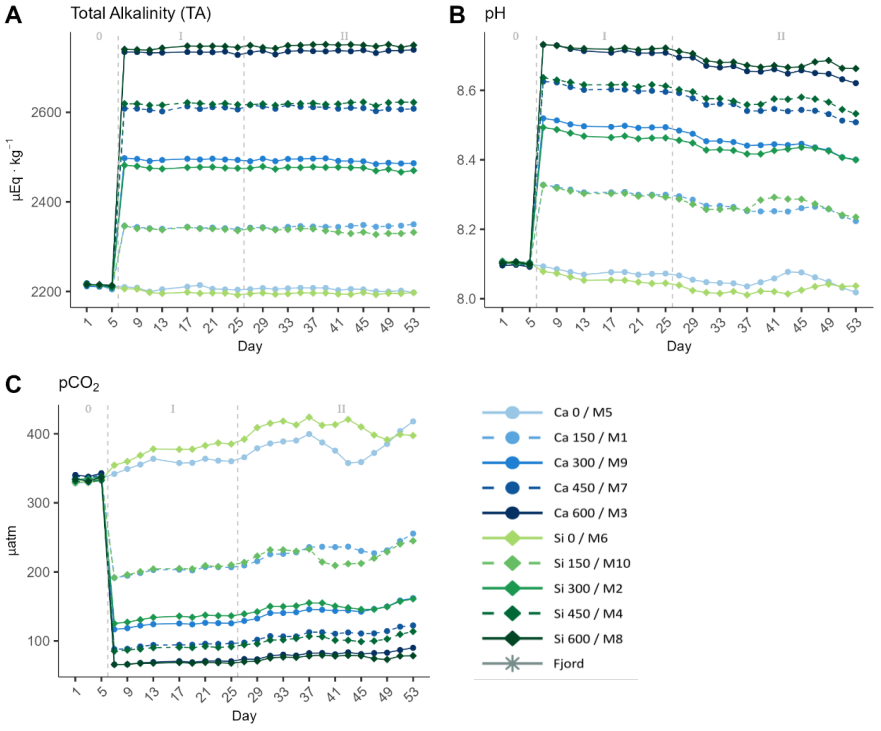

Figure 1. Temporal development of A) Total Alkalinity, B) pH and C) partial pressure of CO_2 (pCO_2) attained throughout the experiment. In the legend, the blue gradient corresponds to the Calcium (Ca) treatments, and the green gradient to the Silicate (Si) based ones, in both cases followed by the target delta TA levels.

Nutrient concentrations (Figure 2) were significantly low at the beginning of the experiment. Conditions that are characteristic of a post-bloom environment. In fact, nitrate (NO_3^-) concentrations were below detection limit during phase I (mean NO_3^- from day 7 - 25 = 0.004 ± 0.035 µM), with silicate ($Si(OH)_4$), in the calcium treatments, and phosphate (PO_4^{-3}) concentrations ranging from 0.06 to 0.44 µM and from 0 to 0.09 µM, respectively. The $Si(OH)_4$ concentration in the silicate based treatments, also in phase I, ranged from 65.9 to 69.8 µM. No $Si(OH)_4$ uptake was observed during this phase. After the nutrient addition on day 26, that depicts the start of phase II, a second addition was carried out on day 28 to correct for stoichiometric differences between mesocosms (Supp. Fig. S1 and Figure 2). Mean $Si(OH)_4$ (in the calcium treatments, no further $Si(OH)_4$ was added in the silicate treatments), NO_3^-, and PO_4^{-3} after addition on day 28 were of 1.07 ± 0.06, 3.62 ± 0.1, and 0.2 ± 0.02 µM respectively.

The average concentrations of the three inorganic nutrients across the silicate and calcium treatments separately on day 29 and on the last day of the experiment, were calculated. The average concentrations for the last day were subtracted to those obtained on day 29 for the two mineral treatments separately. In the calcium treatments, 1.03 ± 0.06 µM, 3.56 ± 0.09 µM and 0.19 ± 0.01 µM of $Si(OH)_4$, NO_3^-, and PO_4^{-3} respectively, were consumed during phase II. In the silicate ones, the decrease in the average NO_3^-, and PO_4^{-3} concentrations observed across all treatments was highly similar (3.67 ± 0.09 µM and 0.19 ± 0.02 µM). However, a steeper decrease of 10.79 ± 1.5 µM of $Si(OH)_4$, compared to that observed for the calcium

https://doi.org/10.5194/egusphere-2024-1776
Preprint. Discussion started: 20 June 2024

treatments, was detected due to the increased availability. Thus, suggesting the community was silicate limited in the calcium treatments, and nitrogen limited in the silicate ones. Additionally, silicate uptake starts to occur later in phase II in the calcium treatments than in the silicate ones. For further details on nutrients dynamics see Ferderer et al. (2023).

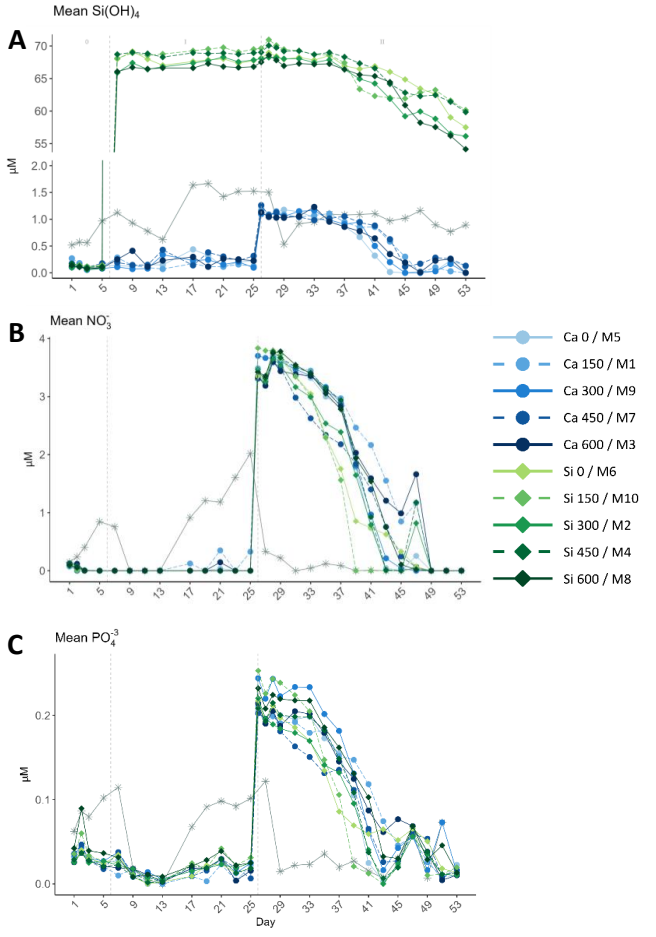

Figure 2. Temporal development of the mean A) silicate ($Si(OH)_4$), B) nitrate (NO_3^-) and C) phosphate (PO_4^{-3}) obtained from triplicate daily measurements throughout the experiment. In the legend, the blue gradient corresponds to the Calcium (Ca) treatments, and the green gradient to the Silicate (Si) based ones, in both cases followed by the target delta TA levels.

3.2 Metabolic rates and chlorophyll a concentration

Before the TA manipulation, mean GP and CR rates were 5.31 ± 0.8 and 1.57 ± 0.3 µmol $O_2 \cdot L^{-1} d^{-1}$ respectively, and the mean Chla concentration was 1.08 ± 0.2 µg $\cdot L^{-1}$ (Figure 3). A slight drop to half of the mentioned GP and Chla, and almost half of the CR rates, was observed right after the addition in all treatments, down to 2.43 ± 0.4 and 0.98 ± 0.5 µmol $O_2 \cdot L^{-1} d^{-1}$ on day 9 (Figure 3). However, no significant linear trends were found in this short-term response phase, nor was there a difference between the two sets of mineral treatments (Figure 4). By day 25, CR accounted for over half of the GP that was at 2.02 ± 0.5

https://doi.org/10.5194/egusphere-2024-1776
Preprint. Discussion started: 20 June 2024

µmol $O_2 \cdot L^{-1} d^{-1}$, while in the Fjord, the GP rate reached a value of over 20 µmol $O_2 \cdot L^{-1} d^{-1}$, and CR was slightly almost 2.5 µmol $O_2 \cdot L^{-1} d^{-1}$. The same pattern as for the GP was observed for the Chla concentration. CR rates recovered fully by day 13 and remained relatively constant ranging between little under 1, and 2 µmol $O_2 \cdot L^{-1} d^{-1}$ throughout this first phase. In the second phase, GP rates in the mesocosms increase. However, when comparing the production and Chla in the fjord and the mesocosms during the blooms, assimilation numbers were much higher in the former than in the latter.

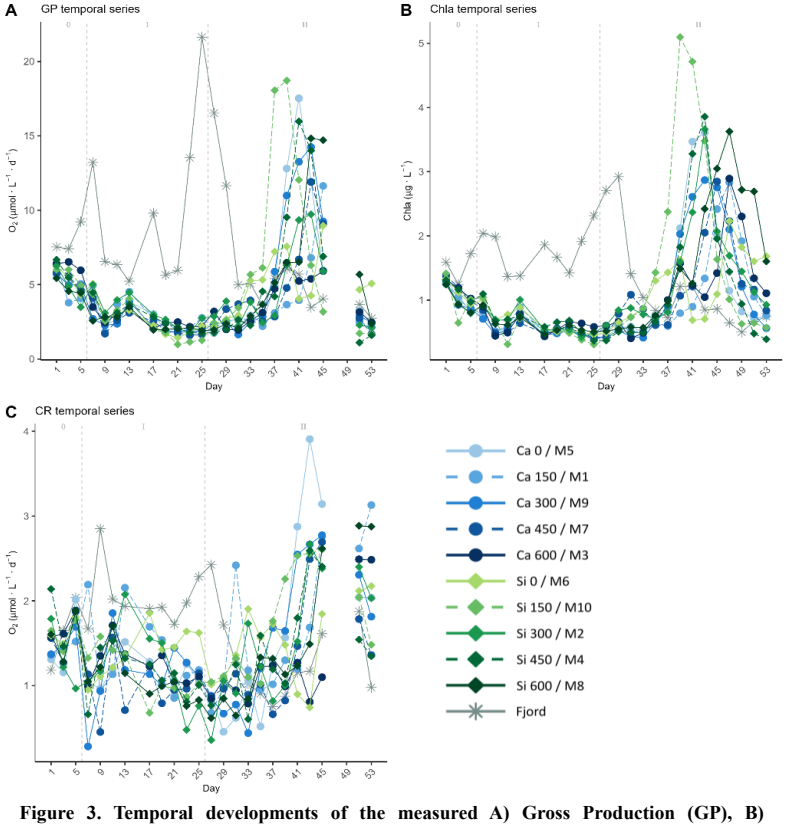

Figure 3. Temporal developments of the measured A) Gross Production (GP), B) Chlorophyll a concentrations and C) Community Respiration (CR), throughout the experiment. In the legend, the blue gradient corresponds to the Calcium (Ca) treatments, and the green gradient to the Silicate (Si) based ones, in both cases followed by the target delta TA levels.

In the temporal series included in the previous figure, no apparent pattern can be discerned. However, when looking at these parameters over time for each mesocosm individually, as seen in Supp. Fig. S3, the low TA treatments are seen to respond to the nutrient addition slightly earlier than the high TA ones. This pattern is portrayed more clearly in Figure 4. The slopes and 95 % confidence intervals obtained from daily linear models of GP and Chla with the ΔTA gradient, as well as the absolute daily values, were plotted over time for the silicate and the calcium treatments separately.

Overall, GP (Figure 4 A and B) and Chla concentrations (Figure 4 C and D) were marginally higher in the silicate-based than in the calcium-based treatments. Additionally, in the silicate treatments both (Figure 4

https://doi.org/10.5194/egusphere-2024-1776
Preprint. Discussion started: 20 June 2024

A and C) augmented earlier than in the calcium ones, showing a negative slope with the ΔTA gradient starting on day 31, which peaked by day 37. Posteriorly, the low TA treatments began to drop, and the GP and Chla concentration in the high TA ones started to increase. Thus, the slope from the mentioned daily linear models reversed, peaking on day 41. In contrast, in the calcium treatments Figure 4 B and D), since the response in the control and low TA mesocosms began 3 sampling days later, the highest negative slope was observed on day 41. Meaning thus that the increase in GP in the silicate based highest treatments corresponded with when the peaks in the low TA calcium ones occurred. Therefore, portraying a delay in the community's response to the nutrient addition that was longer for the calcium treatments, and that followed the TA gradient (Figure 3A and B).

https://doi.org/10.5194/egusphere-2024-1776
Preprint. Discussion started: 20 June 2024

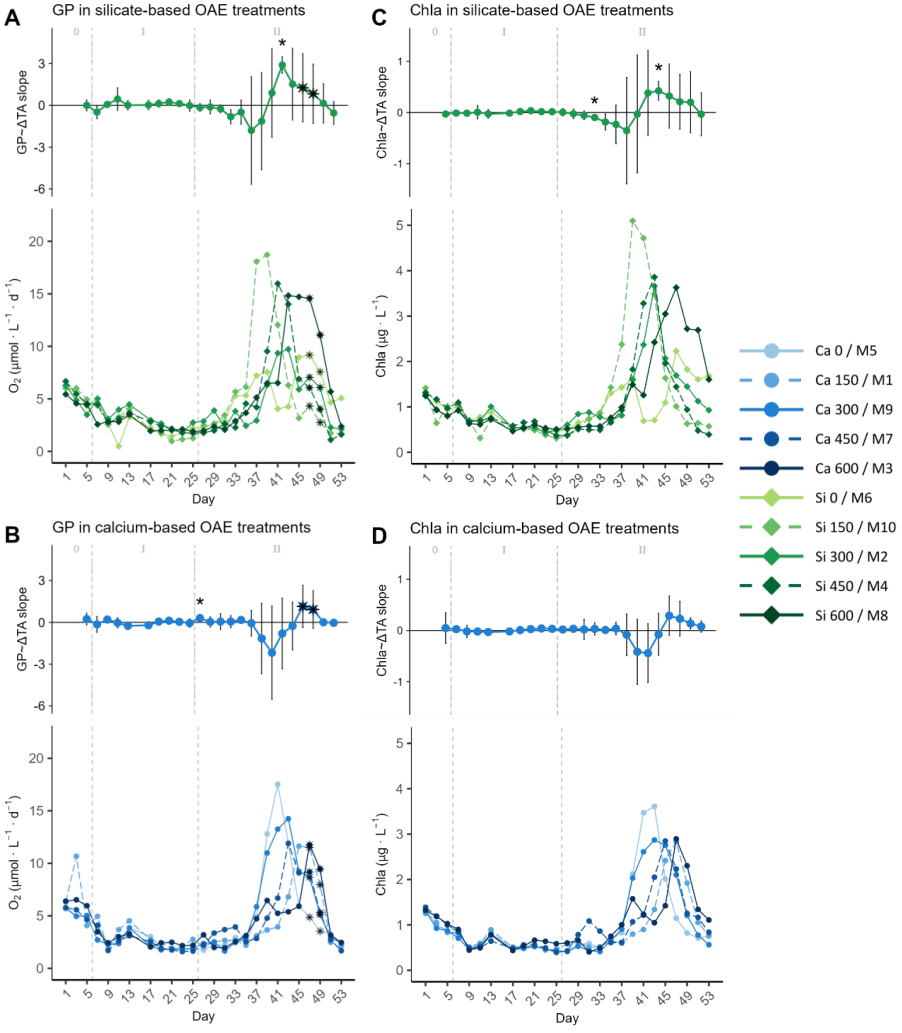

Figure 4. Temporal development of the (top under each letter) delta Total Alkalinity (TA) effect size (slope ± 95% confidence intervals of daily linear models) on, and (bottom within each panel) absolute measurements of (A and B) Gross Production (GP) and (C and D) Chlorophyll a, separated by mineral treatment, where the silicate-based treatments are represented in A and C, and the calcium ones in B and D. The days when a significant relationship (p-values < 0.05) was observed are indicated with a star above the CI bars. The data points marked with a black star on top (days 47 and 49) were estimated by correlating the base-10 logarithm of GP and base-10 logarithm of Chla and using the spearman model equation to calculate the missing GP values. In the legend, the blue gradient corresponds to the Calcium (Ca) treatments, and the green gradient to the Silicate (Si) based ones, in both cases followed by the target delta TA levels.

Due to the COVID outbreak, data for GP on days 47 and 49 could not be obtained. During these days, the Chla concentration in the high TA calcium treatments increased, inverting the relationship with the ΔTA gradient as in the silicate-based treatments. The measured Chla concentrations were correlated with the GP rates and the model equation (Supp. Fig. 4) was used to calculate the missing GP data points. The calculated values are marked with black stars in Figures 4A and B, and all that follow. To calculate the missing CR values, the measured GP and NCP rates were correlated, so that the missing NCP rates could be calculated

https://doi.org/10.5194/egusphere-2024-1776
Preprint. Discussion started: 20 June 2024

with the latter model equation (Supp. Fig. 5), and then subtracted to the previously estimated GP. CR contributed significantly less than NCP to GP during the second phase.

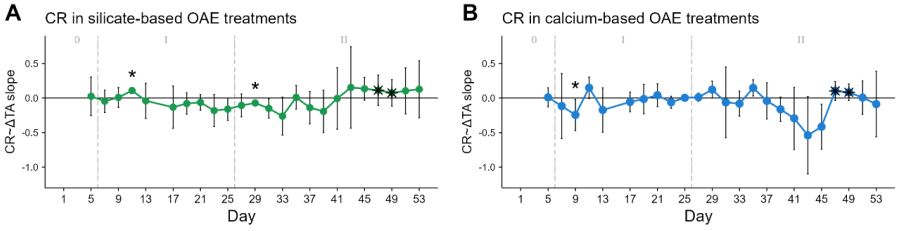

Figure 5. Temporal development of the delta Total Alkalinity (TA) effect size (slope ± 95% confidence intervals of daily linear models) on the Community Respiration (CR) rates for the (left) silicate and (right) calcium-based treatments. The days when a significant relationship (p-values < 0.05) was observed are indicated with a star above the CI bars. The data points marked with a black star on top (days 47 and 49) were estimated by correlating the measured Net Community Production (NCP) to the Gross Production (GP), then using the obtained spearmen model equation to calculate the missing NCP values, and finally subtracting the latter to the calculated GP values. These were estimated using the spearman correlation equation of base-10 logarithm of the measured GP and base-10 logarithm of Chla.

In the silicate treatments, CR did not portray the pattern that was followed by the GP and the Chla concentrations described above (Figure 5A). Nonetheless, it was partially apparent in the CR rates observed in the calcium treatments (Figure 5B). The latter's low TA treatments portrayed an increase in CR around the same time as in terms of GP and, the calculated CR rates that followed showed a slight recovery in the high TA treatments.

3.3 Metabolic balance and assimilation numbers

The metabolic balance was mostly above 1 throughout the experiment (Figure 6). Thus, meaning that overall, the community was in an autotrophic state, even during phase I. Besides, particularly in phase II, the absolute metabolic balance was observed to be slightly higher in the silicate treatments compared to the calcium ones.

https://doi.org/10.5194/egusphere-2024-1776
Preprint. Discussion started: 20 June 2024

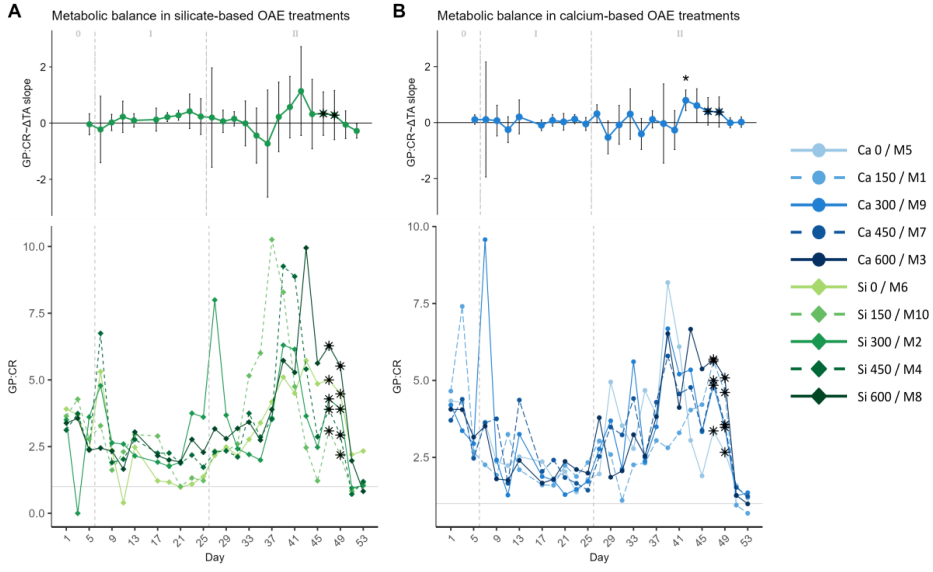

Figure 6. Temporal development of the (top under each letter) ΔTotal Alkalinity (TA) effect size (slope ± 95% confidence intervals of daily linear models) on, and (bottom within each panel) of the calculated metabolic balance (ratio of Gross Production, GP, over Community Respiration, CR), where A) represents the silicate-based treatments, and B) the calcium ones. The days when a significant relationship (p-values < 0.05) was observed are indicated with a star above the CI bars. The data points marked with a black star on top (days 47 and 49) were calculated by dividing estimations of GP and CR. The missing GP values were estimated using the spearman correlation equation of the base-10 logarithm of GP and base-10 logarithm of Chla. Then CR were calculated by correlating the measured Net Community Production (NCP) to the Gross Production (GP), then using the obtained spearmen model equation to calculate the missing NCP values, and finally subtracting the latter to the calculated GP values. In the legend, the blue gradient corresponds to the Calcium (Ca) treatments, and the green gradient to the Silicate (Si) based ones, in both cases followed by the target delta TA levels.

When examining the overtime effect size of the ΔTA, the pattern observed for the Chla and GP described above is only apparent for the metabolic balance in the silicate treatments (Figure 6 A). Although, late in phase II, around the same time as for the silicate treatments, the latter parameter in the high calcium treatments also increased with respect to the low TA ones (Figure 6 B). Additionally, in the silicate treatment set during phase I, and as is evident from the effect size graph in Figure 6 A, a mild positive effect of ΔTA is visible until the nutrient addition.

Further, to see if the pattern observed also translated, to some extent, to the community composition of likely, the microphytoplankton fraction, assimilation numbers based on the GP rates were calculated. GP was chosen due to the low CR rates observed when compared to the NCP, especially during the second phase. But also, because when the NCP is positive, the actual production that is occurring must be at least as much as the CR. The GP normalization using the Chla as a biomass proxy yielded assimilation numbers that remained reasonably constant throughout the experiment and overall, unaffected neither by the mineral treatment, nor by the TA increment. Differences between phases were not apparent either.

https://doi.org/10.5194/egusphere-2024-1776
Preprint. Discussion started: 20 June 2024

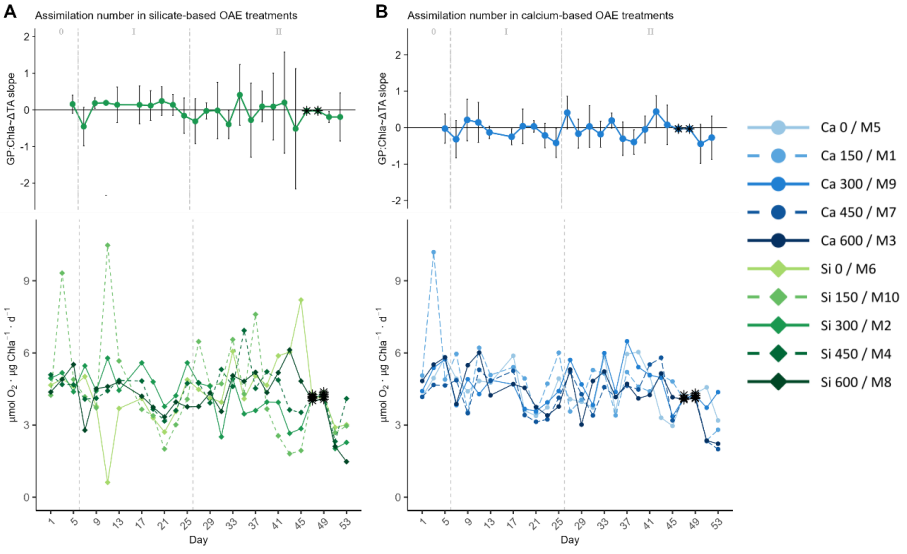

Figure 7. Temporal development of the (top under each letter) delta Total Alkalinity (TA) effect size (slope ± 95% confidence intervals of daily linear models) on, and (bottom within each panel) of the calculated assimilation numbers (ratio of Gross Production, GP, over Chlorophyll a concentration), where A) represents the silicate-based treatments, and B) the calcium ones. The data points marked with a black star on top (days 47 and 49) were calculated because GP could not be measured on those days. The missing GP values were estimated using the spearman correlation equation of the base-10 logarithm of GP and base-10 logarithm of Chla. In the legend, the blue gradient corresponds to the Calcium (Ca) treatments, and the green gradient to the Silicate (Si) based ones, in both cases followed by the target delta TA levels.

4. DISCUSSION

The experiment presented here consisted of the deployment of two separate alkalinity gradients using two OAE strategies based on different minerals: hydrated lime and forsterite. The latter are both being considered for OAE implementation, but no experimental work on their potential effects on natural communities has been undertaken to date. In the present study, simulations were carried out by, instead of using the raw minerals, diluting the elements that conform them separately to reduce the potential effects of confounding variables such as the release of raw mineral impurities.

Large scale equilibrated OAE deployment would require the use of reactors for pre-equilibration (Hartmann et al., 2023) so it would be much more costly, and thus less scalable and feasible. Therefore, CO_2 sequestration was not conducted prior to the alkalinity manipulation in order to evaluate the potential effects of the carbonate chemistry alterations associated with a non-equilibrated OAE deployment. These entailed a persistent increase in pH and decrease in pCO_2, since full natural equilibration did not occur.

In this particular study, the focus was to ascertain whether the microbial community, inhabiting a neritic system, would respond in terms of production and respiration rates during an almost three-month exposure to the aforementioned conditions. Besides, differences in the response to the calcium and silicate inputs caused by the mineral addition simulations mentioned above were expected too. Especially in terms of community composition with calcium-based OAE treatments through the hydrated lime “addition”,

https://doi.org/10.5194/egusphere-2024-1776
Preprint. Discussion started: 20 June 2024

potentially increasing pelagic calcifier abundances, and silicate-based OAE through the forsterite "addition", favoring diatom proliferation. The latter community shifts were predicted to yield distinct responses in terms of absolute community metabolic rates, and production efficiency via clear differences in assimilation numbers over time.

4.1 Response to the carbonate chemistry conditions and to the mineral type

The experiment was started under post-bloom conditions (Figure 2). Nutrient concentrations were low when the treatments were applied. Thus, an initial response in the microbial community production and respiration rates to the TA manipulation was likely concealed by the nutrient limitation. Actually, after a mixing event was simulated on day 26 and 28, a response could be discerned.

The results from the current study show a delay in bloom formation with increasing TA, when such manipulation is non-equilibrated. This delay is, although not significantly, longer in the calcium than in the silicate treatments. Meaning that the low silicate treatments responded slightly earlier to the nutrient addition, than the low calcium ones.

In the past, prior to the emergence of ocean acidification as a focal point in scientific inquiry, several culture experiments simulating high pH/low CO_2 conditions were carried out. For instance, Goldman (1999) carried out 12-day pH-drift, batch culture experiments, with three large diatom species (*Stephanopyxis palmeriana, Ditylum brightwelli and Cosinodiscus* sp.) and found that, when pH rose to above 8.5, growth rates started to decline. Similarly, Hansen (2002) performed 7-day experiments with three dinoflagellate species to evaluate their response in terms of growth rates and community succession. These were exposed to a pH range of 7.5 – 10 applied through the addition of NaOH to simulate the conditions in the Mariager Fjord, Denmark. In these experiments, the three species' growth rates were the highest at pH 7.5, and a decrease to a 20% of the maximum growth rate was observed at pH 8.3-8.5 for *Certaium lineatum*, and at 8.8–8.9 for *Heterocapsa triqueta* and *Prorocentrum minimum.* The latter also showed different tolerance limits, specifically 8.8, 9.5, and 9.6, respectively.

Additionally, despite the lack of data from experiments performed at constant pH at the time, Hansen (2002) compared his results with literature data on 35 species of marine phytoplankton and concluded that there was high variability in their tolerance to high pH. Even within the same family, species-specific tolerance limits could be observed. Most of these species would have been able to grow past the levels reached in the present study, but their growth rates would possibly decrease, at different species-specific levels, in relation to the increased pH (Chen & Durbin, 1994; Hansen, 2002). Therefore, offering the main explanation behind the delay in bloom formation detected here.

High extracellular pH can alter key membrane transport processes and metabolic functions involved in pH regulation (Smith and Raven, 1979). It can also induce changes in cellular amino acid relative composition and overall content (Søderberg and Hansen, 2007). But an key associated variable behind the response in terms of production observed in the present study is the inter-speciation of inorganic carbon caused by the non-equilibrated nature of the TA manipulation. At pH 8, 1% of the DIC is present as CO_2, but at pH 9, this percentage is reduced 10 times over (Hansen, 2002). Additionally, 95% of the carbon fixation in the ocean is undertaken by the photosynthetic carbon-fixation reaction mediated by the RUBISCO (ribulose

https://doi.org/10.5194/egusphere-2024-1776
Preprint. Discussion started: 20 June 2024

bisphosphate carboxylase oxygenase) enzyme, which can only employ CO_2 (Raven, 2000). Thus, besides the pH levels reached here being around 8.7 in the highest treatments (calcium and silicate Δ600 µmol · L^{-1}), which are well above the maximum of 8.2 measured by Omar et al. (2019) in early spring (from 2005 to 2009) along the Norwegian west coast (particularly Raunefjord, Korsfjord, Langenuen, and southern parts of the Hardangerfjord), the associated low pCO_2 attained was likely the detrimental treatment variable. CO_2 is the main substrate for photosynthesis although, in its absence, many marine phytoplankton species adapt by using HCO_3^- through Carbon Concentrating Mechanisms (CCMs). The latter are more energetically costly because they entail the concentration of HCO_3^- at the diffusion range of the plasma membrane, and the catalysis of the HCO_3^- to CO_2 for posterior CO_2 fixation. Thus, these pathways are less efficient, causing reduced growth rates, and the subsequent delay in bloom formation with increasing TA without pre-equilibration (higher pH/lower CO_2 conditions) observed.

Besides the three-day lag noticed for the calcium treatments' response to the nutrient addition with respect to that of the silicate ones, and despite assimilation numbers showing no response to the TA gradient in either case, several differences between the two mineral treatments were noticed. Mildly higher production rates and Chla concentrations were observed in the silicate treatments when compared to the calcium ones. Both silicate and calcium treatment sets' microphytoplankton fractions were likely dominated by diatoms (Ferderer et al., 2023; Kittu et al., 2024, in prep). Small diatoms are usually well adapted to post-bloom conditions due to their favorable surface to volume ratio, an adaptation to low nutrient concentrations (Raven, 1986), and their well-developed CCMs (Chrachri et al., 2018). Additionally, Daniels et al. (2015) studied the phytoplankton community structure dynamics during the early stages of the 2012 North Atlantic spring bloom. They noticed that, in the Norwegian Basin, the diatom community was dominated by nano-sized diatoms. If the same occurred in the present study, acclimation to the carbonate chemistry conditions during phase I, coupled with exposure to high concentrations of silicate in the silicate treatments (positive slopes in daily linear models between ΔTA on GP:CR during phase I; Figure 6 A), would explain the faster response after the nutrient addition and the vast silicate uptake observed (Si:N ~10.7: 3.7 µM), when compared to the calcium treatments. In the latter, the community was silicate limited, in terms of nutrient uptake. All the orthosilicate, as well as the nitrate, introduced to the system were consumed in a ~1: 3.6 µM Si:N ratio. Diatoms have been observed to reduce their silicon requirements by exhibiting frustule thinning if exposed to silicate-limiting conditions to prioritize growth (McNair et al., 2018). In fact, Ferderer et al. (2023) found that diatoms in the silicate treatments were more heavily silicified than in the calcium ones, independently of the TA level. Which could potentially explain the further delayed response to the mixing event simulation and the mildly lower absolute GP and Chla concentration observed in phase II when compared to the silicate treatments.

Further differences between mineral treatments could be inferred in the effect size of ΔTA on CR rates over time, which translated to differences in the effect of ΔTA on metabolic balance. A potential explanation for these results is likely in relation to differences in the phytoplankton community composition between the two sets of treatments. Notably, Ferderer et al. (2023) found that the effect of the mineral on silicification varied between diatom genera in the same experiment. However, even if the community was dominated by diatoms, rapid diatom growth during a spring bloom does not necessarily suppress other non-diatom phytoplankton growth (Lochte et al., 1993; Barber and Hiscock, 2006). The latter may increase in absolute

https://doi.org/10.5194/egusphere-2024-1776
Preprint. Discussion started: 20 June 2024

cell concentrations and in terms of growth rates, but their contribution to the total biomass when diatoms are abundantly present is moderate (Barber and Hiscock, 2006). This would therefore explain why, when GP is normalized to Chla (assimilation numbers), no differences between mineral treatments, even if they occurred, and the response pattern observed in terms of GP and Chla, cannot be inferred in the aforementioned parameters' overtime response (Figure 7).

Lastly, the silicate control behaved differently than expected. The increase in production and in Chla concentrations in the form of a large peak, as in all other treatments after said addition, was not observed. Instead, both in terms of GP and Chla, two small peaks, a half in magnitude when compared to the calcium control, were noted. This difference between the controls was unexpected. This was probably a random response caused by the mesocosm effect. When communities are enclosed, even if initially they are very similar, they are not exactly the same and, over time, they may behave differently. The pre-addition phase allows for acclimation, but it is held as short as possible in order to keep a similar community when the treatment is applied. However, it is still a bias to be taken into consideration.

4.2 Potential implications and future research

Given the novelty of this field and the findings from the current study, we outline herein some of the remaining unresolved research questions. Trophic decoupling between phytoplankton and zooplankton has been observed in a large temperate lake where *Daphnia* resting eggs were unaffected by temperature increase while the phytoplankton spring bloom occurred earlier in the year (Winder and Schindler, 2004). This led to a long-term decline of *Daphnia,* the keystone herbivore, due to the increased mismatch with the spring bloom. The opposite could be expected due to the observed delay in bloom development associated with the non-equilibrated OAE implementation. That is if micro- and mesozooplankton do not respond to the pH levels attained themselves, favoring trophic transfer. In this experiment however, the zooplankton response was not observed due to the late formation of the bloom and the time scale of the experiment. Considering that the transport of particulate organic matter to depth is regulated by the coupling of primary and secondary producers (Wassmann, 1998), thus potentially affecting the OAE's CDR efficiency, this is a key implication that requires further assessment.

Additionally, if the carbonate chemistry conditions were altered under pre-bloom or blooming conditions, the initial shock without prior acclimation may be stronger. It could potentially translate to longer delays in bloom development with increasing TA, and even changes in community composition and overall production efficiency at certain alkalinity levels. Consequently, in turn affecting trophic transfer and carbon export.

Finally, we hypothesize that the delayed response observed in relation to the TA manipulation would likely be amplified if higher non-equilibrated alkalinity additions were deployed. Thus, experiments that look into how and when absolute community metabolic rates respond to stronger OAE deployments, where the threshold in the higher range of the gradient at which a community shift could be induced is, but also if a recovery could occur after a long-term exposure, or after dilution (short-term), are essential if deployment safe limits are to be identified.

https://doi.org/10.5194/egusphere-2024-1776
Preprint. Discussion started: 20 June 2024

5. CONCLUSIONS

The current study presents the results of the first experiment to evaluate the effects of a non-equilibrated, silicate vs calcium based OAE deployment under natural conditions, and at a mesocosm scale, on microbial metabolic rates. The Total Alkalinity (TA) manipulation (a silicate and a calcium based five-step ΔTA gradients 0 – 600 μmol · L^{-1}), without prior CO_2 sequestration, induced a stable increase in pH and a decrease in pCO_2 that lasted until the end of the experiment. The experiment was carried out in a neritic system under post bloom conditions, and a mixing event was simulated roughly halfway through it. After the inorganic nutrient addition, a delay in bloom formation based on Gross and Net Community Production (GP and NCP) rates, and Chlorophyll a (Chla) concentrations, which was longer for the calcium than for the silicate treatment set, in relation to the ΔTA gradient (low TA treatments responded earlier than high TA ones), could be inferred. This response is likely due to the previously reported, species-specific negative relationship between high pH/low pCO_2 conditions and phytoplankton growth rates. The observed system's response is novel, and therefore, further research is necessary to evaluate its potential implications in terms of trophic transfer. Additionally, seasonal differences in the mentioned pattern require further assessment due to the concealment of a potentially more pronounced, short-term response to the TA addition due to the nutrient limitation. We also anticipate this response to become more apparent if higher TA levels are attained. Thus, additional experiments under pre-blooming and blooming conditions to evaluate recovery to more intense carbonate chemistry manipulations are essential to evaluate TA limits, as well as seasonal suitability, for future OAE implementation.

Data availability

The raw data supporting the conclusions of this article will be made available in a public data repository by the authors, without undo reservation.

Author contributions

Experimental concept and design: UR and JA. Direct participation in the experiment: LMS, JA and UR. Data analyses: LMS with input from NHH. Original draft preparation: LMS. Review and editing: All authors.

Financial support

This research has been supported by the Horizon 2020 Research and Innovation Programme project OceanNETs ("Ocean-based Negative Emissions Technologies – analysing the feasibility, risks and cobenefits of ocean-based negative emission technologies for stabilizing the climate", grant no. 869357), and by the EU H2020-INFRAIA's project AQUACOSM ("AQUACOSM: Network of Leading European AQUAtic MesoCOSM Facilities Connecting Mountains to Oceans from the Arctic to the Mediterranean", Project No.: 731065). Further, it was co-financed by the "Agencia Canaria de Investigación, Innovación y Sociedad de la Información" (ACIISI) of the "Consejería de Economía, Conocimiento y Empleo", and by

https://doi.org/10.5194/egusphere-2024-1776
Preprint. Discussion started: 20 June 2024

the "Fondo Social Europeo (FSE) Programa Operativo Integrado de Canarias 2014-2020, Eje 3 Tema Prioritario 74 (85%)".

Competing interests

The authors declare that they have no conflict of interest.

Acknowledgements

The authors would like to express their most sincere gratitude to the entire KOSMOS team at GEOMAR for their invaluable support in managing logistics and, to the technical team for all the hard work building and maintaining the mesocosms during the campaign. Special appreciation is extended to said team's dedication in coordinating on-site research activities and fostering fair data management and exchange. A special thank you goes to Acorayda González from the biological oceanography group (GOB-ULPGC), for helping with the oxygen measurements. Also, we would like to acknowledge Julieta Schneider (GEOMAR) and Kai Shulz (Southern Cross University) for the carbonate chemistry measurements, Juliane Tammen for the inorganic nutrient concentration data, and Leila Kittu (GEOMAR) Xiaoke Xin, Phillip Süßle, and Joaquin Ortiz for the interesting discussions on data interpretation. Finally, we want to thank the University of Bergen for providing the Espegrend Marine Research Field Station to conduct the experiment, and the station's staff for all their assistance throughout.

References

Albright, R., Caldeira, L., Hosfelt, J., Kwiatkowski, L., Maclaren, J. K., Mason, B. M., Nebuchina, Y., Ninokawa, A., Pongratz, J., Ricke, K. L., Rivlin, T., Schneider, K., Sesboüé, M., Shamberger, K., Silverman, J., Wolfe, K., Zhu, K., and Caldeira, K.: Reversal of ocean acidification enhances net coral reef calcification, Nature, 531, 362–365, https://doi.org/10.1038/nature17155, 2016.

Bach, L. T., Gill, S. J., Rickaby, R. E. M., Gore, S., and Renforth, P.: CO2 Removal With Enhanced Weathering and Ocean Alkalinity Enhancement: Potential Risks and Co-benefits for Marine Pelagic Ecosystems, Front. Clim., 1, https://doi.org/10.3389/fclim.2019.00007, 2019.

Barber, R. T. and Hiscock, M. R.: A rising tide lifts all phytoplankton: Growth response of other phytoplankton taxa in diatom-dominated blooms, Global Biogeochem. Cycles, 20, 1–12, https://doi.org/10.1029/2006GB002726, 2006.

Carpenter, C. and: Modifications Employed of the Winkler Method for Determining Dissolved Oxygen in Seawater ; A NASCO Report ', 1966.

Chen, C. Y. and Durbin, E. G.: Effects of pH on the growth and carbon uptake of marine phytoplankton, Mar. Ecol. Prog. Ser., 109, 83–94, https://doi.org/10.3354/meps109083, 1994.

Chen, S. M., Riebesell, U., Schulz, K. G., Von Der Esch, E., Achterberg, E. P., and Bach, L. T.: Temporal dynamics of surface ocean carbonate chemistry in response to natural and simulated upwelling events

https://doi.org/10.5194/egusphere-2024-1776
Preprint. Discussion started: 20 June 2024

during the 2017 coastal El Niño near Callao, Peru, Biogeosciences, 19, 295–312, https://doi.org/10.5194/bg-19-295-2022, 2022.

Chrachri, A., Hopkinson, B. M., Flynn, K., Brownlee, C., and Wheeler, G. L.: Dynamic changes in carbonate chemistry in the microenvironment around single marine phytoplankton cells, Nat. Commun., 9, 1–12, https://doi.org/10.1038/s41467-017-02426-y, 2018.

Czerny, J., Schulz, K. G., Krug, S. A., Ludwig, A., and Riebesell, U.: Technical note: The determination of enclosed water volume in large flexible-wall mesocosms KOSMOS, Biogeosciences, 10, 1937–1941, https://doi.org/10.5194/bg-10-1937-2013, 2013.

Daniels, C. J., Poulton, A. J., Esposito, M., Paulsen, M. L., Bellerby, R., St John, M., and Martin, A. P.: Phytoplankton dynamics in contrasting early stage North Atlantic spring blooms: Composition, succession, and potential drivers, Biogeosciences, 12, 2395–2409, https://doi.org/10.5194/bg-12-2395-2015, 2015.

Dickson, A., Sabine, C., and Christian, J.: Guide to Best Practices for Ocean C02 Measurments, PICES Special Publication 3, 191 pp., 2007.

Feng, E. Y., Koeve, W., Keller, D. P., and Oschlies, A.: Model-Based Assessment of the CO2 Sequestration Potential of Coastal Ocean Alkalinization, Earth's Futur., 5, 1252–1266, https://doi.org/10.1002/2017EF000659, 2017.

Ferderer, A., Schulz, K. G., Riebesell, U., Baker, K. G., Chase, Z., and Bach, L. T.: Investigating the effect of silicate and calcium based ocean alkalinity enhancement on diatom silicification, Biogeosciences Discuss., 1–28, 2023.

Friedlingstein, P., Jones, M. W., O'Sullivan, M., Andrew, R. M., Hauck, J., Peters, G. P., Peters, W., Pongratz, J., Sitch, S., Le Quéré, C., Bakker, D. C. E., Canadell, J. G., Ciais, P., Jackson, R. B., Anthoni, P., Barbero, L., Bastos, A., Bastrikov, V., Becker, M., Bopp, L., Buitenhuis, E., Chandra, N., Chevallier, F., Chini, L. P., Currie, K. I., Feely, R. A., Gehlen, M., Gilfillan, D., Gkritzalis, T., Goll, D. S., Gruber, N., Gutekunst, S., Harris, I., Haverd, V., Houghton, R. A., Hurtt, G., Ilyina, T., Jain, A. K., Joetzjer, E., Kaplan, J. O., Kato, E., Klein Goldewijk, K., Korsbakken, J. I., Landschützer, P., Lauvset, S. K., Lefèvre, N., Lenton, A., Lienert, S., Lombardozzi, D., Marland, G., McGuire, P. C., Melton, J. R., Metzl, N., Munro, D. R., Nabel, J. E. M. S., Nakaoka, S.-I., Neill, C., Omar, A. M., Ono, T., Peregon, A., Pierrot, D., Poulter, B., Rehder, G., Resplandy, L., Robertson, E., Rödenbeck, C., Séférian, R., Schwinger, J., Smith, N., Tans, P. P., Tian, H., Tilbrook, B., Tubiello, F. N., van der Werf, G. R., Wiltshire, A. J., and Zaehle, S.: Global Carbon Budget 2019, Earth Syst. Sci. Data, 11, 1783–1838, https://doi.org/10.5194/essd-11-1783-2019, 2019.

Friedlingstein, P., Jones, M. W., O'Sullivan, M., Andrew, R. M., Bakker, D. C. E., Hauck, J., Le Quéré, C., Peters, G. P., Peters, W., Pongratz, J., Sitch, S., Canadell, J. G., Ciais, P., Jackson, R. B., Alin, S. R., Anthoni, P., Bates, N. R., Becker, M., Bellouin, N., Bopp, L., Chau, T. T. T., Chevallier, F., Chini, L. P., Cronin, M., Currie, K. I., Decharme, B., Djeutchouang, L. M., Dou, X., Evans, W., Feely, R. A., Feng, L., Gasser, T., Gilfillan, D., Gkritzalis, T., Grassi, G., Gregor, L., Gruber, N., Gürses, Ö., Harris, I., Houghton, R. A., Hurtt, G. C., Iida, Y., Ilyina, T., Luijkx, I. T., Jain, A., Jones, S. D., Kato, E., Kennedy, D., Goldewijk, K. K., Knauer, J., Korsbakken, J. I., Körtzinger, A., Landschützer, P., Lauvset, S. K., Lefèvre, N., Lienert,

https://doi.org/10.5194/egusphere-2024-1776
Preprint. Discussion started: 20 June 2024

S., Liu, J., Marland, G., McGuire, P. C., Melton, J. R., Munro, D. R., Nabel, J. E. M. S., Nakaoka, S. I., Niwa, Y., Ono, T., Pierrot, D., Poulter, B., Rehder, G., Resplandy, L., Robertson, E., Rödenbeck, C., Rosan, T. M., Schwinger, J., Schwingshackl, C., Séférian, R., Sutton, A. J., Sweeney, C., Tanhua, T., Tans, P. P., Tian, H., Tilbrook, B., Tubiello, F., Van Der Werf, G. R., Vuichard, N., Wada, C., Wanninkhof, R., Watson, A. J., Willis, D., Wiltshire, A. J., Yuan, W., Yue, C., Yue, X., Zaehle, S., and Zeng, J.: Global Carbon Budget 2021, Earth Syst. Sci. Data, 14, 1917–2005, https://doi.org/10.5194/essd-14-1917-2022, 2022.

Fuss, S., Canadell, J. G., Ciais, P., Jackson, R. B., Jones, C. D., Lyngfelt, A., Peters, G. P., and Van Vuuren, D. P.: Moving toward Net-Zero Emissions Requires New Alliances for Carbon Dioxide Removal, One Earth, 3, 145–149, https://doi.org/10.1016/j.oneear.2020.08.002, 2020.

Gafar, N. A. and Schulz, K. G.: A three-dimensional niche comparison of Emiliania huxleyi and Gephyrocapsa oceanica: Reconciling observations with projections, Biogeosciences, 15, 3541–3560, https://doi.org/10.5194/bg-15-3541-2018, 2018.

Gattuso, J. P., Magnan, A. K., Bopp, L., Cheung, W. W. L., Duarte, C. M., Hinkel, J., Mcleod, E., Micheli, F., Oschlies, A., Williamson, P., Billé, R., Chalastani, V. I., Gates, R. D., Irisson, J. O., Middelburg, J. J., Pörtner, H. O., and Rau, G. H.: Ocean solutions to address climate change and its effects on marine ecosystems, Front. Mar. Sci., 5, https://doi.org/10.3389/fmars.2018.00337, 2018.

Goldman, J. C.: Inorganic carbon availability and the growth of large marine diatoms, Mar. Ecol. Prog. Ser., 180, 81–91, https://doi.org/10.3354/meps180081, 1999.

Grasshof, K., Kremling, K., and Ehrhard, M.: Arsenic , antimony , and germanium , in Methods of Seawater Analysis edited, Wiley-VCH, Weinheim, 274–294, 1999.

Hansen, H. P. and Koroleff, F.: Determination of nutrients, Methods seawater Anal., 159–228, 1999.

Hansen, P. J.: Effect of high pH on the growth and survival of marine phytoplankton: implications for species succession, 28, 279–288, 2002.

Hartmann, J., Suitner, N., Lim, C., Schneider, J., Marín-Samper, L., Arístegui, J., Renforth, P., Taucher, J., and Riebesell, U.: Stability of alkalinity in ocean alkalinity enhancement (OAE) approaches - consequences for durability of CO2storage, Biogeosciences, 20, 781–802, https://doi.org/10.5194/bg-20-781-2023, 2023.

Harvey, L. D. D.: Mitigating the atmospheric CO2 increase and ocean acidification by adding limestone powder to upwelling regions, J. Geophys. Res. Ocean., 113, 1–21, https://doi.org/10.1029/2007JC004373, 2008.

Holmes, R. M., Aminot, A., Kérouel, R., Hooker, B. A., and Peterson, B. J.: A simple and precise method for measuring ammonium in marine and freshwater ecosystems, Can. J. Fish. Aquat. Sci., 56, 1801–1808, https://doi.org/10.1139/f99-128, 1999.

IPCC: Global warming of 1.5°C, 228–231 pp., 2018.

IPCC, I. P. on C. C. (Ed.): Global Carbon and Other Biogeochemical Cycles and Feedbacks, in: Climate Change 2021 – The Physical Science Basis: Working Group I Contribution to the Sixth Assessment Report of the Intergovernmental Panel on Climate Change, Cambridge University Press, Cambridge, 673–816,

https://doi.org/10.5194/egusphere-2024-1776
Preprint. Discussion started: 20 June 2024

https://doi.org/DOI: 10.1017/9781009157896.007, 2023.

Jones, D. C., Ito, T., Takano, Y., and Hsu, W. C.: Spatial and seasonal variability of the air-sea equilibration timescale of carbon dioxide, Global Biogeochem. Cycles, 28, 1163–1178, https://doi.org/10.1002/2014GB004813, 2014.

Kheshgi, H. S.: Sequestering atmospheric carbon dioxide by increasing ocean alkalinity, Energy, 20, 915–922, https://doi.org/10.1016/0360-5442(95)00035-F, 1995.

Lee, J.-Y., J. Marotzke, G. Bala, L. Cao, S. Corti, J.P. Dunne, F. Engelbrecht, E. Fischer, J.C. Fyfe, C. Jones, A. Maycock, J. Mutemi, O. Ndiaye, S. Panickal, and T. Zhou: Future Global Climate: Scenario-Based Projections and Near-Term Information, 553–672 pp., https://doi.org/10.1017/9781009157896.006.553, 2021.

Lewis, E. and Wallace, D.: Program Developed for CO2 System Calculations ORNL/CDIAC-105, Carbon Dioxide Information Analysis Centre, 1998.

Lochte, K., Ducklow, H. W., Fasham, M. J. R., and Stienen, C.: Plankton succession and carbon cycling at 47°N 20°W during the JGOFS North Atlantic Bloom Experiment, Deep Sea Res. Part II Top. Stud. Oceanogr., 40, 91–114, https://doi.org/https://doi.org/10.1016/0967-0645(93)90008-B, 1993.

Marín-Samper, L., Arístegui, J., Hernández-Hernández, N., Ortiz, J., Archer, S. D., Ludwig, A., and Riebesell, U.: Assessing the impact of CO2 equilibrated ocean alkalinity enhancement on microbial metabolic rates in an oligotrophic system, EGUsphere, 2024, 1–29, 2024.

McNair, H. M., Brzezinski, M. A., and Krause, J. W.: Diatom populations in an upwelling environment decrease silica content to avoid growth limitation, Environ. Microbiol., 20, 4184–4193, https://doi.org/10.1111/1462-2920.14431, 2018.

Montserrat, F., Renforth, P., Hartmann, J., Leermakers, M., Knops, P., and Meysman, F. J. R.: Olivine Dissolution in Seawater: Implications for CO2 Sequestration through Enhanced Weathering in Coastal Environments, Environ. Sci. Technol., 51, 3960–3972, https://doi.org/10.1021/acs.est.6b05942, 2017.

Omar, A. M., Skjelvan, I., Erga, S. R., and Olsen, A.: Aragonite saturation states and pH in western Norwegian fjords: Seasonal cycles and controlling factors, 2005-2009, Ocean Sci., 12, 937–951, https://doi.org/10.5194/os-12-937-2016, 2019.

Paul, A. J. and Bach, L. T.: Universal response pattern of phytoplankton growth rates to increasing CO2, New Phytol., 228, 1710–1716, https://doi.org/10.1111/nph.16806, 2020.

Raven, J. A.: Physiological consequences of extremely small size for autotrophic organisms in the sea, Canandian Bull. Fish. Aquat. Sci., 214, 1–70, 1986.

Raven, J. A.: Limits on growth rates, Nature, 11, 438–443, 2000.

Raven, J. A. and Johnston, A.: Mechanisms of inorganic-carbon acquisition in marine phytoplankton and their implications for the use of other resources concentration on growth and photosynthe- sis by marine phytoplankton organisms has been little investigated relative to the effects me, 36, 1991.

Renforth, P. and Henderson, G.: Assessing ocean alkalinity for carbon sequestration, Rev. Geophys., 55,

https://doi.org/10.5194/egusphere-2024-1776
Preprint. Discussion started: 20 June 2024

636–674, https://doi.org/10.1002/2016RG000533, 2017.

Riebesell, U., Wolf-Gladrow, D. A., and Smetacek, V.: Carbon dioxide limitation of marine phytoplankton growth rates, Nature, 361, 249–251, https://doi.org/10.1038/361249a0, 1993.

Riebesell, U., Czerny, J., Von Bröckel, K., Boxhammer, T., Büdenbender, J., Deckelnick, M., Fischer, M., Hoffmann, D., Krug, S. A., Lentz, U., Ludwig, A., Muche, R., and Schulz, K. G.: Technical Note: A mobile sea-going mesocosm system - New opportunities for ocean change research, Biogeosciences, 10, 1835–1847, https://doi.org/10.5194/bg-10-1835-2013, 2013.

Schuiling, R. D. and Krijgsman, P.: Enhanced weathering: An effective and cheap tool to sequester CO 2, Clim. Change, 74, 349–354, https://doi.org/10.1007/s10584-005-3485-y, 2006.

Smith, F. A. and Raven, J. A.: AND ITS REGULATION, 1979.

Søderberg, L. M. and Hansen, P. J.: Growth limitation due to high pH and low inorganic carbon concentrations in temperate species of the dinoflagellate genus Ceratium, 351, 103–112, https://doi.org/10.3354/meps07146, 2007.

Taucher, J., Bach, L. T., Boxhammer, T., Nauendorf, A., Achterberg, E. P., Algueró-Muñiz, M., Arístegui, J., Czerny, J., Esposito, M., Guan, W., Haunost, M., Horn, H. G., Ludwig, A., Meyer, J., Spisla, C., Sswat, M., Stange, P., Riebesell, U., Aberle-Malzahn, N., Archer, S., Boersma, M., Broda, N., Büdenbender, J., Clemmesen, C., Deckelnick, M., Dittmar, T., Dolores-Gelado, M., Dörner, I., Fernández-Urruzola, I., Fiedler, M., Fischer, M., Fritsche, P., Gomez, M., Grossart, H. P., Hattich, G., Hernández-Brito, J., Hernández-Hernández, N., Hernández-León, S., Hornick, T., Kolzenburg, R., Krebs, L., Kreuzburg, M., Lange, J. A. F., Lischka, S., Linsenbarth, S., Löscher, C., Martínez, I., Montoto, T., Nachtigall, K., Osma-Prado, N., Packard, T., Pansch, C., Posman, K., Ramírez-Bordón, B., Romero-Kutzner, V., Rummel, C., Salta, M., Martínez-Sánchez, I., Schröder, H., Sett, S., Singh, A., Suffrian, K., Tames-Espinosa, M., Voss, M., Walter, E., Wannicke, N., Xu, J., and Zark, M.: Influence of ocean acidification and deep water upwelling on oligotrophic plankton communities in the subtropical North Atlantic: Insights from an in situ mesocosm study, Front. Mar. Sci., 4, https://doi.org/10.3389/fmars.2017.00085, 2017.

Wassmann, P.: Retention versus export food chains: processes controlling sinking loss from marine pelagic systems, in: Eutrophication in Planktonic Ecosystems: Food Web Dynamics and Elemental Cycling: Proceedings of the Fourth International PELAG Symposium, held in Helsinki, Finland, 26--30 August 1996, edited by: Tamminen, T. and Kuosa, H., Springer Netherlands, Dordrecht, 29–57, https://doi.org/10.1007/978-94-017-1493-8_3, 1998.

Welschmeyer, N. A.: Fluorometric analysis of chlorophyll a in the presence of chlorophyll b and pheopigments, Limnol. Oceanogr., 39, 1985–1992, https://doi.org/10.4319/lo.1994.39.8.1985, 1994.

Winder, M. and Schindler, D. E.: Climate change uncouples trophic interactions in an aquatic ecosystem, Ecology, 85, 2100–2106, https://doi.org/10.1890/04-0151, 2004.

Xin, X., Faucher, G., and Riebesell, U.: Phytoplankton Response to Increased Nickel in the Context of Ocean Alkalinity Enhancement, Biogeosciences Discuss., 2023, 1–15, 2023.

Zeebe, R. E. and Wolf-Gladrow, D.: CO2 in seawater: equilibrium, kinetics, Isot. Elsevier Sci. BV,

https://doi.org/10.5194/egusphere-2024-1776
Preprint. Discussion started: 20 June 2024

Amsterdam, Netherlands, 2001.

710 .